

Photocatalytic Degradation of Rhodamine B using CuS-doped ZnS under Visible Light Irradiation

Rachel Mugumo*, Shepherd M. Tichapondwa, Evans M. N. Chirwa

Water Utilisation and Environmental Engineering Division, Department of Chemical Engineering,
 University of Pretoria, Pretoria 0002.
rachelmugumo@gmail.com

This study investigates the photocatalytic activity of CuS/ZnS in the degradation of Rhodamine B, an azo dye in textile wastewater generated through processing operations in textile industries which provides significant socioeconomic benefits. Nanoporous nanocomposites were synthesised via a one-pot thermal decomposition method which exhibited efficient photocatalytic activity. The microstructure and composition of the prepared catalyst was characterized using Scanning Electron Microscopy (SEM), Transmission Electron Microscopy (TEM), Energy-dispersive X-ray Spectroscopy (EDX) and X-Ray Diffraction (XRD). The degradation results showed that coupling pristine ZnS with the highly photosensitive CuS improved the photocatalytic degradation efficiency from 67 % to 88 % in 4 h under solar irradiation. This result clearly depicts the degradation efficacy improvement of ZnS when doped with CuS in rhodamine B degradation using visible light irradiation.

1. Introduction

Water contamination from industrial production has attracted a lot of attention as water is critical in sustaining all life forms. Dyes, heavy metals, and persistent organic pollutants (POPs) are a result of anthropogenic activities, and some are predominant in nature. Their presence in the environment even in minute quantities can pose detrimental health effects such as chronic toxicity, neurological and developmental disorders (Saravanan et al., 2021). Textile industries use azo dyes which are highly water soluble, to meet colour requirements and these industries generate approximately 17-20 % of industrial wastewater. Generated textile wastewater impacts the quality of the aquatic system, recipient water bodies, environmental biodiversity, and human health such as skin irritation, headache, lung problems, nausea, and congenital malformation (Al-Mamun et al., 2019). Traditional conventional methods such as membrane separation, decolourisation, natural aerobic treatment and chemical coagulation have been widely applied in the treatment of textile wastewater, but have experienced drawbacks such as long processing times, chemical instability, high operational costs, separation difficulties and high sludge generation (Ichipi et al, 2021 a). The variability and complexity of textile effluents promotes the implementation of advanced water recovery systems such as flocculation/ coagulation, membrane and biological processes and Advanced Oxidation Processes (AOPs) (Paździor et al., 2019). Commonly used chemical oxidation techniques are suitable for lowering and removal of high organic pollutant concentrations; however, facing the limitation of incomplete mineralisation (Le et al., 2019). The present environmental and energy issues evoke high demand in efficient utilisation of sustainable renewable energy that offers a green, free, safe, and abundant resource such as sunlight. The solar spectrum constitutes of about 5 % UV, 45 % visible and 50 % near-infrared (NIR) light (Jiang et al., 2018).

Most semiconductor photocatalytic systems are developed to conduct solar driven reactions in organic pollutant degradation in wastewater (Zhong et al., 2020). Photocatalytic reactions generally follow three processes: (i) generation of electron/hole pairs from photon absorption, (ii) charge separation and active site migration on surface of photocatalyst, and (iii) redox reactions (oxidation and reduction) mediated by photogenerated e⁻/h⁺ pairs (Huang et al., 2020).

Semiconductor metal sulphides composites have unique physicochemical properties making a widespread potential in applications such as solar cells, drug delivery, sensors, catalysis, and environmental pollution both

air and water (Wang et al., 2014). Transition-metal chalcogenides such as ZnS and CuS have been extensively studied due to their excellent photochemical and luminescent properties (Wang et al., 2016). ZnS is a prominent versatile material that acts as an effective catalyst due to its environmental friendliness, low toxicity, good optical properties, simple preparation, and high light absorbing properties (Varghese, 2021). ZnS however has a wide band gap of about 3.72 eV for its cubic phase and 3.77 eV for its hexagonal phase, it absorbs UV light accounting for only 4 % of total sunlight (Yu et al., 2010) and its fast recombination of photogenerated pairs limits its practical approach (Wang et al., 2016). On the other hand, CuS is a highly effective visible-light stable p-type semiconductor photocatalyst in wastewater/ pollutant treatment due to its environmental friendliness and adjustable narrow band gap (Wang et al., 2014) which is stoichiometry dependent for instance, the band gap for CuS is 2.2 eV, Cu_{1.8}S is 1.5 eV and Cu₂S is 1.2 eV (Yu, 2010). However, CuS has rapid recombination of photogenerated electron/ hole pairs which restricts its degradation efficiency improvement as a photocatalyst (Wang et al., 2014) and is highly susceptible to photocorrosion, nonetheless encapsulation by the large band gap shell of ZnS prevents the oxidation of CuS (Thuy et al., 2014). Coupling CuS to ZnS results in the formation of a heterojunction between the compounds which lowers the band gap energy to allow visible light usage and is also considered to speed up the rate of photoinduced charge separation thereby enhancing photocatalytic activity (Lu et al., 2019). The valence band of CuS is higher and the conduction band lower than ZnS which results in type I band alignment with photogenerated electron/ hole pairs injected into CuS continuously. ZnS is restricted in the UV region (Wang et al., 2014) and doping with CuS improves its visible light photocatalytic degradation efficacy thus ZnS prevents CuS photocorrosion (Thuy et al., 2014) and moreover provides extensive absorption range thus exhibiting enhanced photocatalytic degradation of rhodamine B (Wang et al., 2016).

As far as I know, research has been done on the degradation of rhodamine B under UV irradiation. Herein we report a new synthesis and characterisation of nanoporous CuS/ZnS nanoparticles through solid phase one pot synthesis. The photocatalytic performance of the CuS, ZnS and binary CuS/ZnS was tested and compared under visible light irradiation using rhodamine B as the model organic pollutant.

2. Experimental

2.1 Materials

Copper (II) nitrate trihydrate (copper precursor) and thiourea (sulphur precursor) for the synthesis of CuS/ZnS nanocomposite were purchased from Sigma-Aldrich (St Louis, MO, United States). Zinc nitrate hexahydrate (zinc precursor) was purchased from Glassworld (Johannesburg, South Africa). All reagents were used without further purification. Deionised water was used as a solvent during the study.

2.2 Synthesis

The CuS/ZnS composite catalyst was synthesised using a simple solid phase method at a temperature of 400 °C. Appropriate amounts of Zn(NO₃)₂·6H₂O, (NH₂)₂CS and Cu(NO₃)₂·3H₂O were weighed in the ratio 4:1:0.2, respectively. This mixture was added to a crucible and thoroughly mixed before calcination at 400 °C for 5 h. The obtained product was ground using a pastel and mortar yielding a powdered photocatalyst. Pristine CuS was synthesised using copper II nitrate trihydrate and thiourea: and ZnS using zinc nitrate hexahydrate and thiourea following the same procedure.

2.3 Characterisation

XRD samples were analyzed using a PANalytical X'Pert Pro powder diffractometer in θ - θ configuration with an X'Celerator detector and variable divergence- and fixed receiving slits with Fe filtered Co-K α radiation ($\lambda=1.789\text{\AA}$). The mineralogy was determined by selecting the best-fitting pattern from the ICSD database to the measured diffraction pattern, using X'Pert Highscore plus software. SEM and EDX, and TEM images were captured on a Zeiss Ultra PLUS FEG SEM and JOEL JEM 2100F TEM respectively.

2.4 Photocatalytic activity

The photocatalytic activities of CuS, ZnS and binary CuS/ZnS composite was investigated by monitoring the photodegradation of rhodamine B diluted in deionized water under visible light irradiation. The experimental set-up comprised of a box unit with a cubic size of (92 × 70 × 70) cm³ fitted with three 18 W fluorescent day lamps which served as a source of visible light irradiation. All tests were performed using 10 g/L catalyst loading added to 100 ml of 5 mg/L rhodamine B solution. The suspension was stirred for 30 minutes in the dark to allow for adsorption-desorption equilibrium prior to 4 hours of visible light irradiation. Aliquots of 2 ml were extracted every 30 minutes and subsequently centrifuged for 10 minutes at 9,000 rpm. The collected solution was filtered using 0.45 μm simplepure microfilters and the samples were measured at a wavelength of 554 nm using a Labotec UV/Vis Lightwave II spectrophotometer. The degradation efficiency was determined using the equation 1.

$$\% \text{ Degradation} = \frac{(C_0 - C_t)}{C_0} \times 100 \quad (1)$$

Where C_0 is the initial concentration and C_t if the final concentration of rhodamine B.

3. Results and discussion

3.1 Characterisation

Catalyst Phase Analysis

Figure 1 shows the XRD pattern of prepared ZnS, CuS and CuS/ZnS nanoparticles. The sharp and narrow peaks are an indication of relatively high purity and crystallinity. The similarity in the XRD spectra of the pristine ZnS and CuS/ZnS composite catalysts was attributed to the low concentration of CuS used for doping. The theoretical ratio of CuS to ZnS based on the synthesis procedure was expected to be 0.2:4. The surprising patterns above indicate the presence of their respective oxides [ZnO (JCPDS 36-1451); CuO (JCPDS 02-1040)] in given sulphides [ZnS (JCPDS 05-0492); CuS (JCPDS 78-2391)]. The presence of oxides might have resulted from open air synthesis of the photocatalyst which was performed without the use of a vacuum.

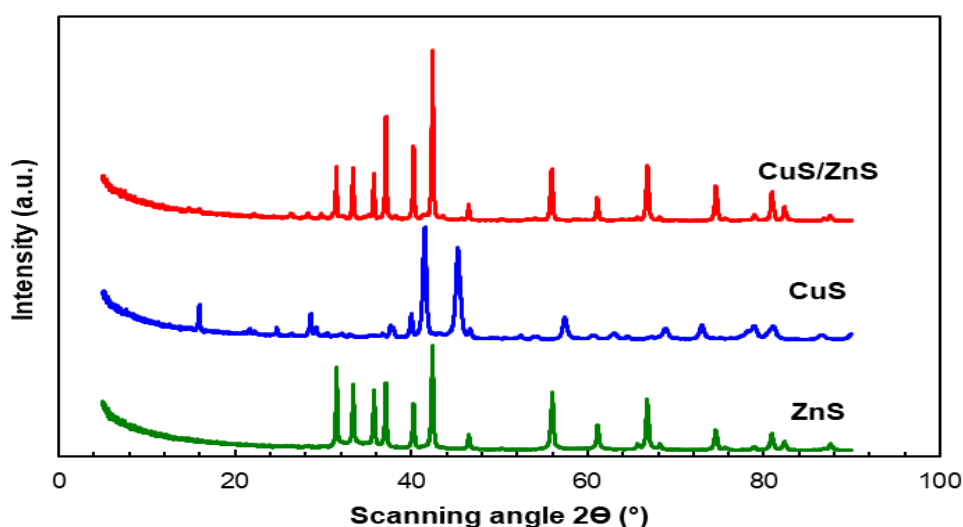


Figure 1: XRD analysis for ZnS, CuS and CuS/ZnS.

Catalyst Surface Characterisation

SEM and TEM were used to analyse and capture morphologies of ZnS, CuS and CuS/ZnS as shown in Figure 2. Figure 2a, 2b and 2c illustrate SEM images for ZnS, CuS and CuS/ZnS as nanoporous agglomerate micropores. Furthermore, Figure 3 a-c further illustrate TEM images of ZnS, CuS and CuS/ZnS as nanoparticles which resemble clustered nanoplates and nanospheres. Synthesis reaction temperature directly affects specific surface area, crystallite size and pore structure (Yu et al., 2009).

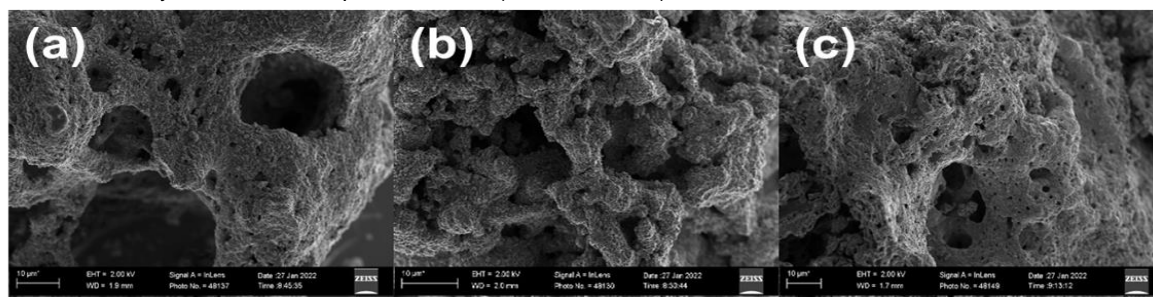


Figure 2: SEM images of (a) ZnS, (b) CuS and (c) CuS/ZnS, respectively.

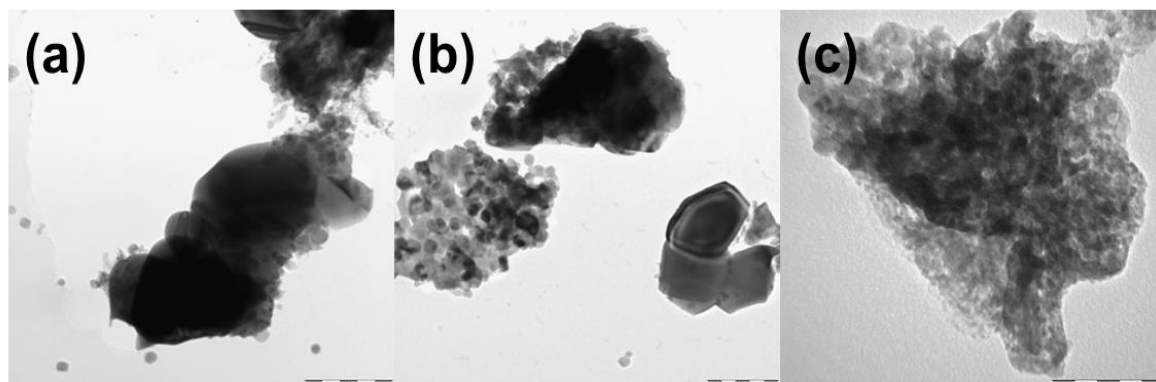


Figure 3: TEM images of (a) ZnS, (b) CuS and (c) CuS/ZnS, respectively.

Element Analysis

Figure 4 shows the EDX spectra analysis for the constituent elements detected in the catalyst namely Zn, S and Cu as 73.84 %, 10.58 % and 6.22 % respectively. The remaining 9.25 % consisted of O which further proves the presence of oxides in the nanocomposite. This EDX spectra proves the presence of Cu in the CuS/ZnS since the XRD spectra was inconclusive and dominated by ZnS.

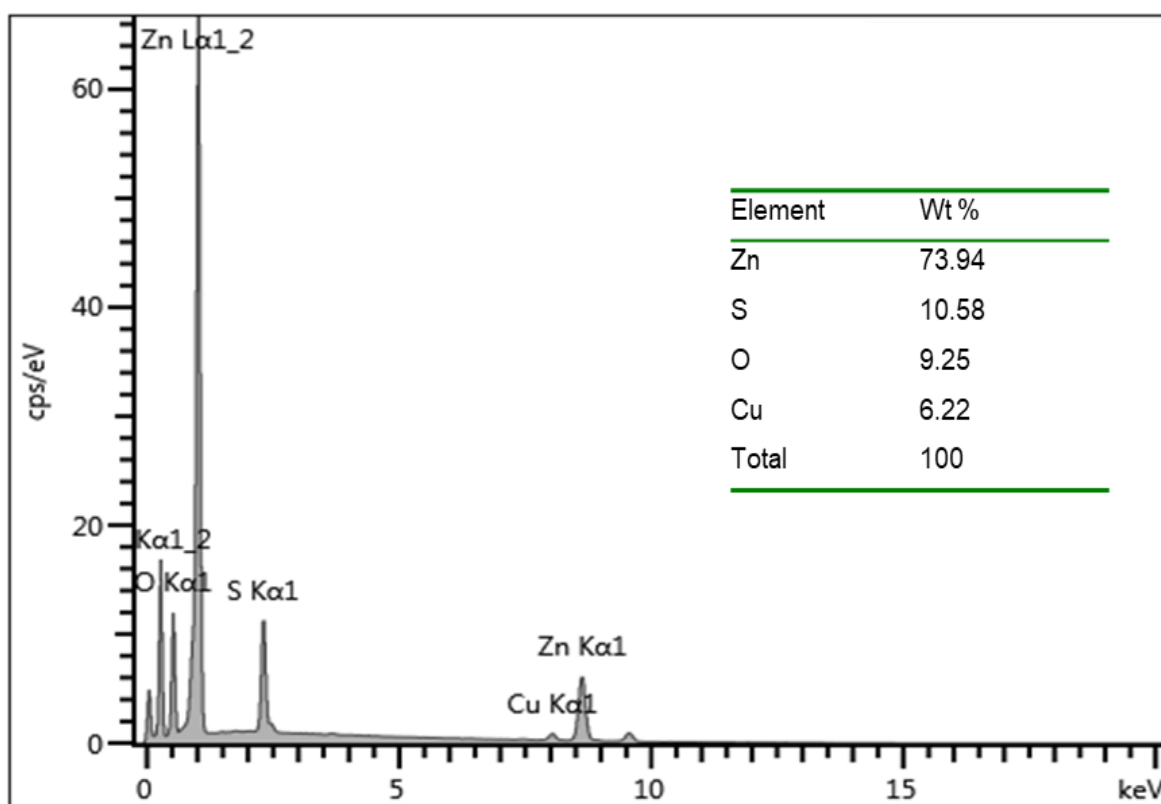


Figure 4: EDX spectra of CuS/ZnS nano powder and its accompanying map sum spectrum showing catalyst constituents.

3.2 Photocatalytic activity

The photodegradation of the prepared photocatalyst was investigated on its ability to degrade rhodamine B in the presence of visible light. A control experiment was carried out to test the effect of visible light alone (photolysis) and the catalyst alone (adsorption) on rhodamine B. The photolysis test resulted in 0 % degradation indicating no detectable degradation in the absence of the catalyst, while the adsorption test (without light)

showed significant dye removal of 63 % reporting the adsorption-desorption equilibrium at that state. CuS/ZnS gives 88 % removal under photocatalytic conditions as compared to 63 % under adsorption conditions. Adsorption-desorption equilibrium is reached after the initial 30 minutes in the dark which reported CuS, ZnS and CuS/ZnS degradation as 23 %, 40 % and 45 % respectively. Figure 5 illustrates that CuS, ZnS and CuS/ZnS degradation activity under visible light for 4 h was 91 %, 67 % and 88 % respectively. Although all catalysts exhibit photocatalytic activity, ZnS had the least degradation percentage which suggests the wide band gap limitation. Meanwhile CuS and CuS/ZnS achieved significant degradation. This result can be compared with the report on modification of ZnO nanoparticles by doping with Ag₂S in the photocatalytic degradation of phenol under visible light irradiation. Upon doping the catalyst composite exhibited an improved activity compared to the primary ZnO nanoparticle (Ichipi et al., 2021 b). CuS/ZnS showed its potential in commercial application as it completely degraded the pollutant in a further experiment carried over 24 hours in visible light irradiation.

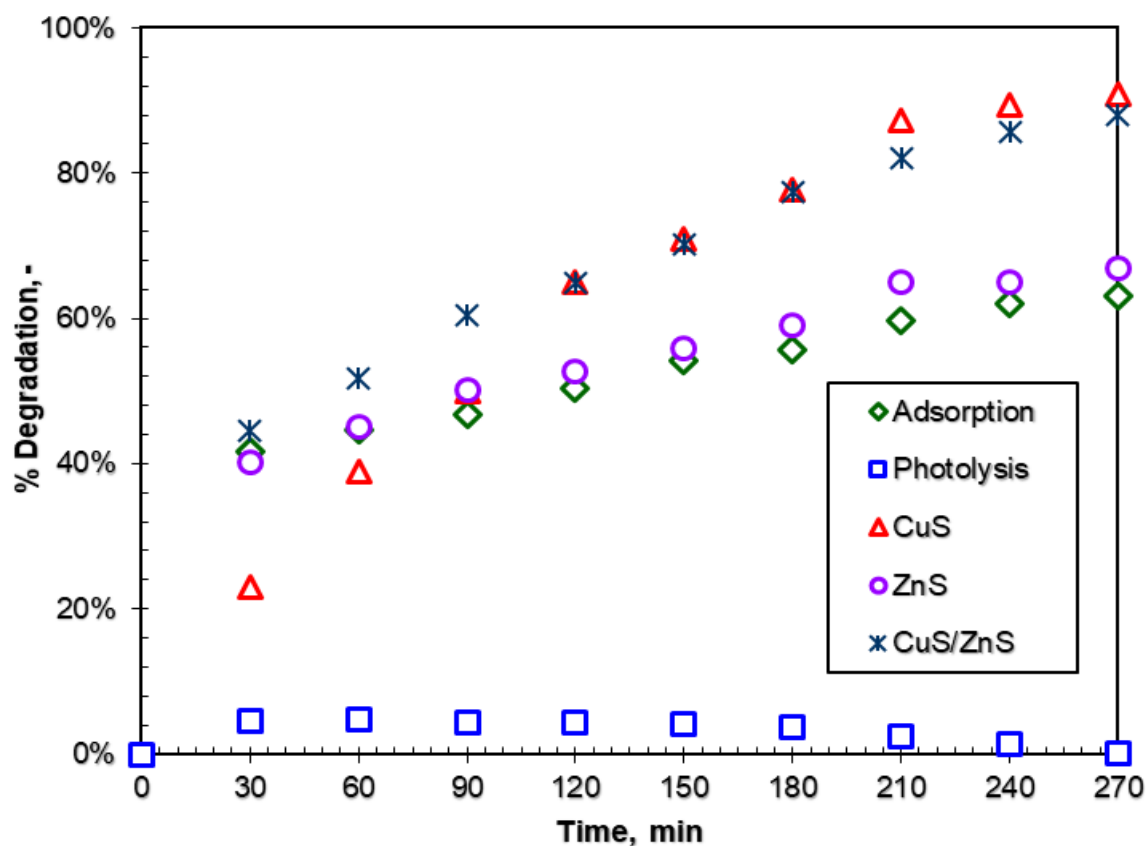


Figure 5: Rhodamine B degradation under visible light irradiation.

4. Conclusions

This study investigated the photoactivity of ZnS doped with CuS nanoparticles fabricated via one-pot thermal decomposition method in the removal of rhodamine B under visible light. The prepared photocatalysts exhibit clear photocatalytic activity in photocatalytic removal and decolourisation of rhodamine B. The physicochemical characteristics of the prepared nanocomposites were determined using XRD, SEM, TEM and EDX. The results prove that doping ZnS with CuS promotes synergistic interaction between both materials by reducing the rate of photogenerated electron/hole pair recombination and lowering the band gap to broaden visible light absorption spectrum.

Acknowledgments

This work is based on research financially supported by the National Research Fund (NRF) of South Africa (Grant numbers: EQP180503325881, TTK18024324064) and Rand Water Chair in Water Utilisation awarded to Prof. Evans M.N. Chirwa and Prof. Shepherd M. Tichapondwa.

References

- Al-Mamun M.R., Kader S., Khan M.Z.H., 2019, Photocatalytic activity improvement and application of UV-TiO₂ photocatalysis in textile wastewater treatment: A review, *Journal of Environmental Chemical Engineering*, 7(5), 103248.
- Harish S., Archana J., Navaneethan M., Ponnusamy S., Singh A., Gupta V., Aswal D.K., Ikeda H., Hayakawa A., 2017, Synergetic effect of CuS/ZnS nanostructures on photocatalytic degradation of organic pollutant under visible light irradiation, *RSC Advances*, 79550, 34366–34375.
- Huang H., Pradhan B., Hofkens J., Roeffaers M.B.J., Steele J.A., 2020, Solar-Driven Metal Halide Perovskite Photocatalysis: Design, Stability, and Performance, *ACS Energy Letters*, 5(4), 1107–1123.
- Ichipi E.O., Tichapondwa S.M., Chirwa E.M.N., 2021 a, Photocatalytic activity of visible-light-driven ternary Ag/Ag₂S/ZnO nanocomposites for phenol degradation in water, *Chemical Engineering Transactions*, 86, 817.
- Ichipi E.O., Tichapondwa S.M., Chirwa E.M.N., 2021 b, Facile synthesis and characterisation of nanosized ZnO modified with Ag₂S for visible-light-induced phenol degradation, *Chemical Engineering Transactions*, 84, 7–12.
- Le M.V.L., Ho T.N.S., Nguyen T.T., Pham T.H.T., Ngo M.T., 2020, Photocatalytic degradation of phenol in aqueous solutions using TiO₂/SiO₂ composite, *Chemical Engineering Transactions*, 78, 427.
- Li D., Yu S.H., Jiang H.L., 2018, From UV to Near-Infrared Light-Responsive Metal–Organic Framework Composites: Plasmon and Upconversion Enhanced Photocatalysis, *Advanced Materials*, 30(27), 1–7.
- Lin S.H., Chen M.L., 1997, Treatment of textile wastewater by-chemical methods for reuse, *Water Research*, 31(4), 868–876.
- Lu J., Zhang J., Chen Q., Liu H., 2019, Porous CuS/ZnS microspheres derived from a bimetallic metal-organic framework as efficient photocatalysts for H₂ production, *Journal of Photochemistry and Photobiology A: Chemistry*, 380, 111853.
- Paździor K., Bilińska L., Ledakowicz S., 2019, A review of the existing and emerging technologies in the combination of AOPs and biological processes in industrial textile wastewater treatment, *Chemical Engineering Journal*, 376, 120597.
- Saravanan A., Karishma S., Jeevanantham S., Gyathri B., Bharathi V.D., Kumar P.S., Vo D.N., 2021, Photocatalysis for removal of environmental pollutants and fuel production: a review, *Environmental Chemistry Letters*, 19(1), 441–463.
- Thuy U.T.D., Liem Q., Parlett C.M.A., Lalev G.M., Wilson K., 2014, Synthesis of CuS and CuS/ZnS core/shell nanocrystals for photocatalytic degradation of dyes under visible light, *Catalysis Communications*, 44, 62–67.
- Varghese J., 2021, CuS–ZnS decorated graphene nanocomposites: Synthesis and photocatalytic properties, *Journal of Physics and Chemistry of Solids*, 156, 109911.
- Wang L., Chen H., Xiao L., Huang J., 2016, CuS/ZnS hexagonal plates with enhanced hydrogen evolution activity under visible light irradiation, *Powder Technology*, 288(3), 103–108.
- Wang X., Li Y., Wang M., Chen M., Zhao Y., 2014, Synthesis of tunable ZnS–CuS microspheres and visible-light photoactivity for rhodamine B, *New Journal of Chemistry*, 38(9), 4182–4189.
- Yu J., Zhang J., Liu S., 2010, Ion-exchange synthesis and enhanced visible-light photoactivity of CuS/ZnS nanocomposite hollow spheres, *Journal of Physical Chemistry C*, 114(32), 13642–13649.
- Yu X., Yu J., Cheng B., Huang B., 2009, One-pot template-free synthesis of monodisperse zinc sulfide hollow spheres and their photocatalytic properties, *Chemistry - A European Journal*, 15(27), 6731–6739.
- Zhong S., Xi Y., Wu S., Liu Q., Zhao L., Bai S., 2020, Hybrid cocatalysts in semiconductor-based photocatalysis and photoelectrocatalysis, *Journal of Materials Chemistry A*, 8(30), 14863–14894.